Notch promotes recurrence of dormant tumor cells following HER2/neu-targeted therapy

Daniel L. Abravanel,[1,2] George K. Belka,[1,2] Tien-chi Pan,[1,2] Dhruv K. Pant,[1,2] Meredith A. Collins,[1,2] Christopher J. Sterner,[1,2] and Lewis A. Chodosh[1,2,3]

[1]Department of Cancer Biology, [2]Abramson Family Cancer Research Institute, and [3]Department of Medicine, Perelman School of Medicine, University of Pennsylvania, Philadelphia, Pennsylvania, USA.

Breast cancer mortality is principally due to recurrent tumors that arise from a reservoir of residual tumor cells that survive therapy. Remarkably, breast cancers can recur after extended periods of clinical remission, implying that at least some residual tumor cells pass through a dormant phase prior to relapse. Nevertheless, the mechanisms that contribute to breast cancer recurrence are poorly understood. Using a mouse model of recurrent mammary tumorigenesis in combination with bioinformatics analyses of breast cancer patients, we have identified a role for Notch signaling in mammary tumor dormancy and recurrence. Specifically, we found that Notch signaling is acutely upregulated in tumor cells following HER2/neu pathway inhibition, that Notch signaling remains activated in a subset of dormant residual tumor cells that persist following HER2/neu downregulation, that activation of Notch signaling accelerates tumor recurrence, and that inhibition of Notch signaling by either genetic or pharmacological approaches impairs recurrence in mice. Consistent with these findings, meta-analysis of microarray data from over 4,000 breast cancer patients revealed that elevated Notch pathway activity is independently associated with an increased rate of recurrence. Together, these results implicate Notch signaling in tumor recurrence from dormant residual tumor cells and provide evidence that dormancy is a targetable stage of breast cancer progression.

Introduction

Improvements in the early detection of breast cancers — coupled with advances in surgery, radiotherapy, and adjuvant therapy — have led to substantial increases in 5-year survival rates for breast cancer patients over the past 50 years. Nevertheless, breast cancer remains the leading cause of cancer-related deaths among women worldwide (1). The majority of these deaths are due to disease relapse after a variable period of clinical remission following treatment. The kinetics of breast cancer recurrence, which may occur up to 25 years after treatment of the primary tumor, imply that at least some breast cancers pass through a phase of dormancy prior to relapse (2–5).

While the vast majority of tumor cells are typically eliminated by surgery, radiation therapy, and adjuvant hormonal therapy or chemotherapy, residual tumor cells frequently survive. Minimal residual disease (MRD) in the form of disseminated tumor cells (DTCs) is present in more than a third of patients at the time of diagnosis, and the presence of DTCs is strongly associated with both disease-free survival and overall survival (6). Similarly, the persistence of DTCs in breast cancer patients following therapy is also associated with an increased risk of relapse (7, 8). Although the biological properties of DTCs have been challenging to study, DTCs in breast cancer patients have been reported to be Ki-67–negative, suggesting that these cells may reside in a dormant state (9, 10). Together, these observations suggest that MRD may serve as a reservoir of dormant tumor cells that can ultimately give rise to recurrent tumors.

While recurrence is perhaps the most important determinant of clinical outcome, the cellular and molecular mechanisms underlying this stage of cancer progression remain poorly defined. In particular, little is known about the signaling pathways that permit residual neoplastic cells to survive in a dormant state and eventually resume growth. Unfortunately, detailed examination of the molecular and cellular mechanisms that contribute to cellular dormancy and recurrence in breast cancer has been limited by difficulties in obtaining clinical samples from patients with MRD and recurrent cancers. There is also the challenge of accurately modeling these complex biological processes in vivo. To overcome these limitations, our laboratory has developed genetically engineered mouse models that recapitulate key features of breast cancer progression, including spontaneous recurrence arising from dormant MRD that persists following therapy (11–16).

In *MMTV-rtTA;TetO-HER2/neu* (*MTB/TAN*) mice, treatment with doxycycline induces HER2/neu signaling in the mammary epithelium, which in turn drives the formation of invasive adenocarcinomas. Upon doxycycline withdrawal and resultant oncogene downregulation, primary tumors regress to a nonpalpable state as a consequence of oncogene addiction. However, a small population of surviving tumor cells persists. Following a variable period of cellular dormancy, residual tumor cells re-enter the cell cycle and give rise to recurrent tumors in a stochastic manner. In line with clinical observations that HER2/neu-positive primary tumors can give rise to HER2/neu-negative residual disease (17, 18) and recurrences (19) following therapy, recurrence in this preclinical mouse model occurs in the absence of HER2/neu expression. This behavior parallels clinical observations in which resistance to HER2/neu targeted therapies can occur through activation of compensatory pathways (20, 21).

Conflict of interest: The authors have declared that no conflict of interest exists.
Submitted: February 13, 2014; **Accepted:** April 13, 2015.
Reference information: *J Clin Invest*. 2015;125(6):2484–2496. doi:10.1172/JCI74883.

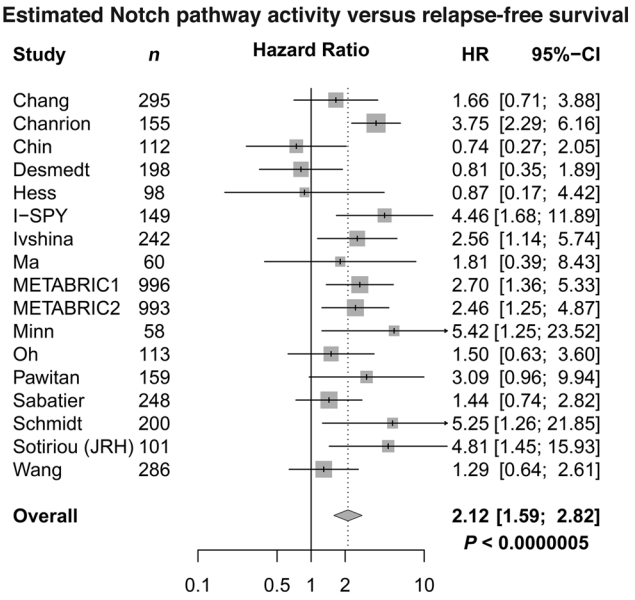

Figure 1. Elevated Notch signaling is associated with decreased relapse-free survival in women with breast cancer. Forest plot representation of meta-analysis on hazard ratios for 5-year relapse-free survival as a function of estimated NOTCH1 pathway activity for 4,463 breast cancer patients across 17 individual datasets using a Notch pathway activity signature. Names and sizes of data sets, HR (center of square), and 95% CIs (horizontal line) are shown for each dataset. Sizes of squares are proportional to weights used in meta-analysis. The overall HRs (dashed vertical lines) and associated CIs (lateral tips of diamond) are shown for the random-effects model. Solid vertical line indicates no effect. The HRs represent the change in risk over half of the full range of estimated pathway activity. The overall *P* value was calculated using a *z*-test on the pooled hazard ratio estimate.

Accumulating data support a role for the Notch pathway in the pathogenesis and progression of human breast cancer. Recurrent gene rearrangements resulting in constitutive NOTCH1 activation have been identified in patients with estrogen receptor–negative (ER-negative) adenocarcinomas of the breast (22), and constitutive activation of Notch signaling in transgenic mice results in the formation of mammary tumors (23–27). Recent data also implicate Notch signaling in resistance to chemotherapy, hormone therapy and targeted therapy in breast cancer cell lines (28). Additionally, positive staining for the intracellular domain of NOTCH1 (NICD1) has been reported to be associated with an increased risk of recurrence in a series of 50 patients with ductal carcinoma in situ (29). Furthermore, elevated expression of *NOTCH1* and *JAG1* mRNAs in primary breast cancers has been associated with poor overall survival in a cohort of 184 patients, with coexpression of *NOTCH1* and *JAG1* mRNAs associated with the highest risk of relapse (30). However, whether Notch plays a functional role in breast cancer recurrence has not been addressed.

In the present study, we employed computational interrogation of breast cancer patient datasets and genetically engineered mouse models for HER2/neu-targeted therapy to elucidate a role for Notch signaling in breast cancer recurrence. Our observations that Notch signaling is associated with a decrease in recurrence-free survival in breast cancer patients, that Notch signaling is upregulated following HER2/neu downregulation, and that inhibition of Notch signaling impairs recurrence of dormant tumor cells implicate Notch signaling as a potential mechanism through which tumor cells evade therapy and recur in breast cancer patients. Our findings identify dormancy as a distinct, rate-limiting, and targetable stage of tumor progression and suggest a new therapeutic approach to the clinical problem of MRD and recurrence.

Results

Notch pathway activity is associated with an increased risk of recurrence in women with breast cancer. To investigate the potential role of Notch in breast cancer recurrence, we first developed a gene-expression signature reflecting Notch activation in mammary epithelial cells. We generated *MMTV-rtTA;TetO-NICD1* (*MTB/TICNX*) transgenic mice that conditionally express NICD1 in the mammary epithelium upon doxycycline administration, and we performed gene expression profiling following 96 hours of doxycycline treatment. As anticipated, canonical Notch targets such as *Hey1* and *Hey2* were acutely upregulated following NICD1 induction (Supplemental Figure 1A; supplemental material available online with this article; doi:10.1172/JCI74883DS1). In parallel, we compared expression profiles of human breast cancer cell lines (31) with and without activating *NOTCH1* gene rearrangements (22). A 72-gene signature was derived from the intersection of the differentially expressed gene lists generated from these 2 data sets (Supplemental Figure 1B and Supplemental Table 1).

Using a previously described scoring method for estimating pathway activity from gene expression data (32), we validated the performance of this Notch signature on independent gene-expression datasets. The signature accurately identified Notch activation in an independent cohort of *MTB/TICNX* mice induced for 48 hours (Supplemental Figure 1C), increases in Notch activity in MCF-10A cells transduced with increasingly potent *NOTCH1* alleles (ref. 32 and Supplemental Figure 1D), activation of Notch signaling in human T-ALL cell lines bearing Notch pathway-activating mutations (ref. 30 and Supplemental Figure 1E), and inhibition of Notch signaling in human T-ALL cell lines treated with a γ-secretase inhibitor (GSI; refs. 33–36 and Supplemental Figure 1F).

We next used this Notch pathway signature to classify human breast cancers according to their predicted levels of Notch activity and asked whether Notch signaling was associated with recurrence-free survival in women with breast cancer. Meta-analysis of data from 17 studies, including 4,463 patients, revealed a robust association between elevated Notch activity and reduced recurrence-free survival (Figure 1; $P < 5 \times 10^{-7}$). Furthermore, while estimated Notch activity was higher in subsets of breast cancers associated with poor clinical outcomes — including basal-like tumors, ER-negative tumors, and high-grade tumors — its association with recurrence-free survival was independent of these prognostic factors in multivariate analyses, and it also remained predictive of recurrence within these high-risk subgroups (Supplemental Figures 2 and 3). These findings suggest that elevated Notch pathway activity is associated with an increased risk of tumor recurrence in breast cancer patients.

Notch signaling is upregulated acutely following HER2/neu downregulation. In light of the strong association between Notch path-

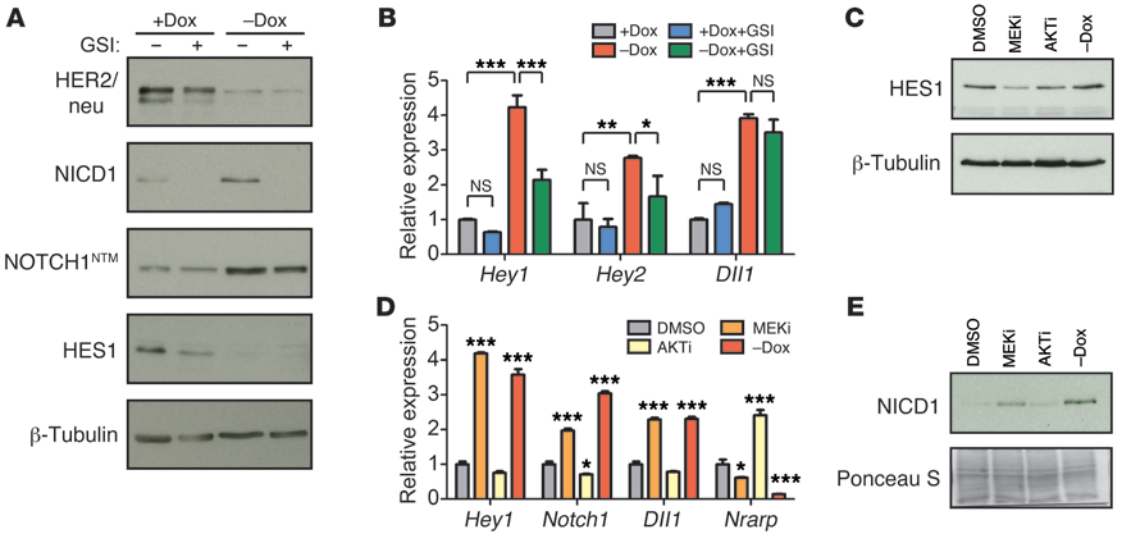

Figure 2. HER2/neu downregulation activates Notch signaling. (**A**–**E**) Western blot and qRT-PCR analyses of Notch signaling components in HER2/neu-dependent primary tumor cells derived from *MTB/TAN* mice: (**A** and **B**) 48 hours after doxycycline withdrawal with and without GSI treatment. (**C**–**E**) Treatment for 4 hours (**C**) or 48 hours (**D** and **E**) with MEKi (PD0325901), AKTi (MK 2206), or doxycycline withdrawal. Data in **B** and **D** are shown as the mean ± SD. $^*P < 0.05$, $^{**}P < 0.01$, and $^{***}P < 0.001$ by 1-way ANOVA followed by the Bonferroni (**B**) or Dunnett (**D**) multiple comparisons tests; $n = 3$. Western blot results are representative of 3 different experiments.

way activity and relapse-free survival in breast cancer patients, we hypothesized that Notch signaling might play a functional role in mammary tumor recurrence. It has been suggested that resistance of human breast cancer cell lines to HER2/neu inhibition can be mediated, at least in part, by activation of Notch signaling in vitro (37) and in xenograft models (38). However, the mechanisms underlying this proposed association are unknown.

First, we used the above Notch pathway signature to address whether HER2/neu blockade alters Notch signaling. Applying our bioinformatics approach to published microarray data from SKBR3 cells, which are $ER^-/PR^-/HER2^+$ (39), we found that Notch pathway activity increased with elevating doses of lapatinib (Supplemental Figure 4A). Next, to determine whether Notch activation following HER2/neu inhibition is evolutionarily conserved, we downregulated HER2/neu in vitro in oncogene-dependent primary tumor cells derived from *MTB/TAN* mice by removing doxycycline from the media. This revealed that HER2/neu downregulation was accompanied by acute upregulation of NICD1, *Hey1*, and *Hey2* in a GSI-sensitive manner, confirming that HER2/neu downregulation results in acute Notch pathway activation (Figure 2, A and B). While levels of NOTCH1 and *Dll1* also increased, these changes were not GSI sensitive, suggesting that they occurred upstream of Notch activation. Importantly, parallel experiments in SKBR3 cells revealed a similar pattern of alterations in *HEY1*, *HEY2*, and *DLL1* levels, suggesting that the mechanisms of crosstalk between HER2/neu and Notch signaling identified in HER2/neu-driven mouse tumor cells may also be operative in HER2-amplified human breast cancer cells (Supplemental Figure 4B).

To assess the contribution of signaling pathways downstream of HER2/neu, we performed analogous experiments, in which the effects of HER2/neu downregulation were compared with those resulting from treatment with inhibitors of RAS/MAPK or AKT signaling. While AKT inhibition had little effect on *Hey1*, *Notch1*, or *Dll1* levels, MEK inhibition closely paralleled the effects of HER2/neu downregulation on these Notch signaling components in *MTB/TAN* primary tumor cells (Figure 2, C–E, and Supplemental Figure 5, A and B). Consistent with this, treatment with a selective ERK1/2 inhibitor also increased NICD levels (Supplemental Figure 5C). In contrast, increased Notch signaling was not observed in SKBR3 cells upon MEK inhibition, suggesting that more than one signaling pathway downstream of HER2/neu may be capable of mediating crosstalk with Notch signaling (data not shown).

HER2/neu represses Notch signaling through HES1 and NRARP. Unexpectedly, HES1 and *Nrarp* expression decreased following HER2/neu downregulation or MEK inhibition (Figure 2, A, C, and D). Although both are canonical Notch targets — and behaved as such in our experiments — evidence exists suggesting that HES1 may also be upregulated through activation of receptor tyrosine kinases, including signaling downstream of FGF and ErbB family members (40–43). Indeed, we found that *Hes1* and *Nrarp* were each downregulated within 6 hours of doxycycline withdrawal and rapidly upregulated by re-addition of doxycycline, suggesting that these genes may be directly regulated by HER2/neu in addition to Notch signaling (Figure 3A).

Of note, HES1 and NRARP have each been reported to inhibit Notch signaling, by either repressing DLL1 expression (44) or inhibiting NICD-mediated activation of target genes (45), respectively. Therefore, we determined the impact of enforced NRARP or HES1 expression on Notch signaling in *MTB/TAN* tumor cells (Figure 3, B and C, and Supplemental Figure 6, A and B). While HER2/neu deinduction led to downregulation of HES1 and upregulation of *Dll1* and *Hey1* in control cells, increases in *Dll1* and *Hey1* expression were attenuated by enforced HES1 expression. Enforced NRARP expression also decreased *Hey1* upregulation upon HER2/neu downregulation. These observations suggest that HES1 and NRARP negatively regulate Notch signaling.

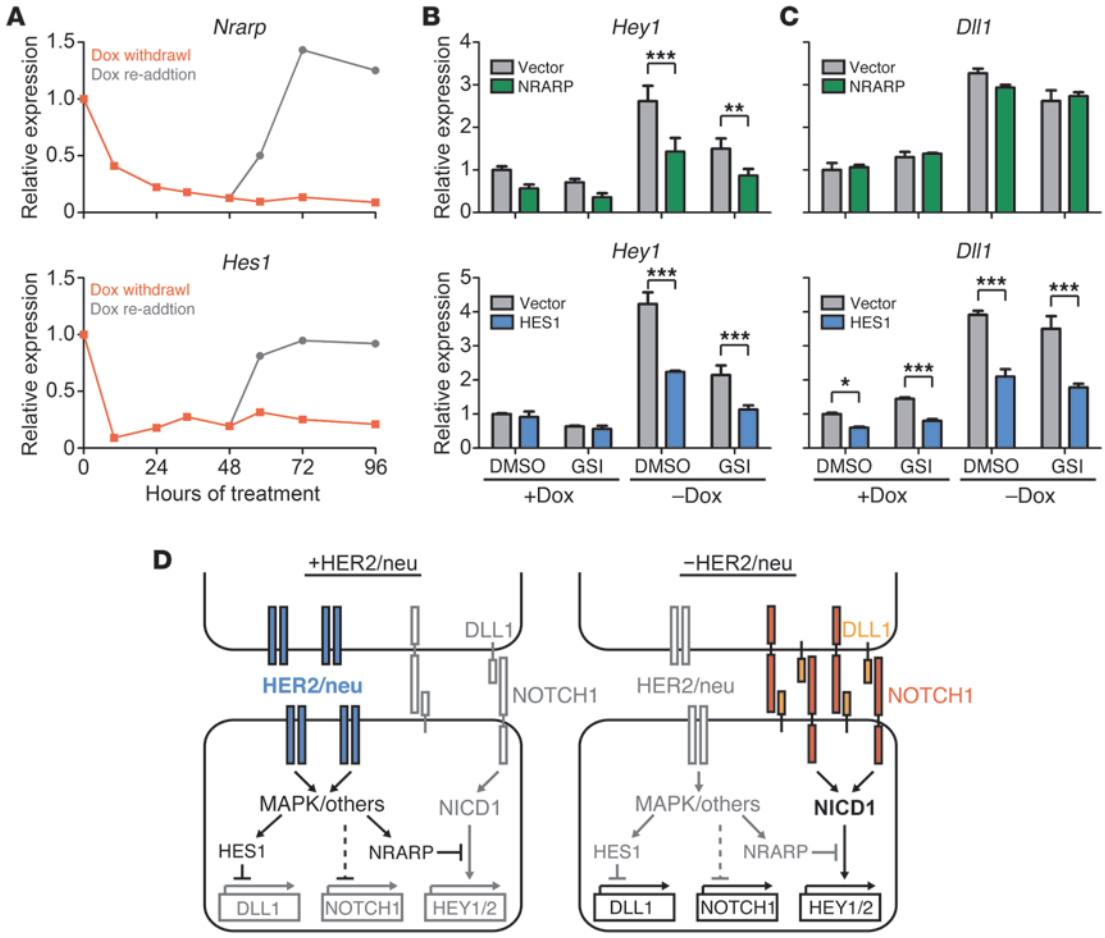

Figure 3. HER2/neu represses Notch signaling through induction of HES1 and NRARP. (**A**) qRT-PCR for *Nrarp* or *Hes1* after doxycycline withdrawal with or without re-addition of doxycycline after 48 hours. Data are representative of 3 different experiments. (**B** and **C**) qRT-PCR for (**B**) *Hey1* or (**C**) *Dll1* expression 48 hours after doxycycline withdrawal with and without GSI treatment in cells transduced with empty vector, NRARP (top), or HES1 (bottom) expression constructs. (**D**) Model for crosstalk between HER2/neu and Notch signaling. MAPK and other signaling pathways downstream of HER2/neu repress DLL1 expression through upregulation of HES1, and they repress NOTCH1 expression. They further attenuate activation of Notch targets through upregulation of NRARP. Downregulation of HER2/neu abrogates this repression, thereby allowing activation of NOTCH1 by DLL1 and upregulation of Notch targets, including HEY1 and HEY2. Data in **B** and **C** are shown as the mean ± SD. $^*P < 0.05$, $^{**}P < 0.01$, and $^{***}P < 0.001$ by 2-way ANOVA followed by the Bonferroni multiple comparisons test; $n = 3$.

In aggregate, these data are consistent with a model in which HES1 and NRARP regulate crosstalk between the HER2/neu and Notch signaling pathways (Figure 3D). In the presence of HER2/neu signaling, activation of signaling pathways — including the MAPK signaling pathway — blocks Notch signaling, at least in part by upregulation of negative regulators of Notch signaling, HES1 and NRARP. Accordingly, inhibition of HER2/neu signaling results in downregulation of HES1 and NRARP, thereby abrogating this repression and allowing activation of Notch1 by DLL1 and upregulation of Notch targets, including HEY1 and HEY2.

Activation of Notch signaling promotes tumor recurrence. We hypothesized that induction of Notch signaling following HER2/neu inhibition might contribute to tumor recurrence. To address this possibility, we first determined the effect that activating or repressing Notch signaling had on the clonogenic survival of *MTB/TAN* tumor cells by expressing constitutively active NICD1, or a dominant-negative *MAML* allele (dn*MAML*), and then downregulating HER2/neu (refs. 46, 47, and Supplemental Figure 6, C and D). In control experiments in which HER2/neu expression was maintained by inclusion of doxycycline in the medium, activation or inhibition of Notch signaling altered colony size but did not affect the number of colonies that formed. In contrast, in the absence of HER2/neu signaling, Notch pathway activation rescued colony formation and, conversely, Notch pathway inhibition impaired colony formation (Figure 4).

Next, to determine the impact of Notch activation on the recurrence of HER2/neu-induced mammary tumors in vivo, we used *MTB/TAN* tumor cells transduced with NICD1 in a doxycycline-inducible orthotopic mouse model (16). Primary tumor cells expressing control or Notch1 gain-of-function constructs were injected into the mammary fat pads of recipient *nu/nu* mice maintained on doxycycline. Following primary tumor formation in the presence of HER2/neu signaling, HER2/neu downregulation induced by doxycycline withdrawal was used to model HER2/neu-targeted therapy. All tumors regressed to a nonpalpable state, irrespective of NICD1 expression (data not shown). However, the rate of recurrence of

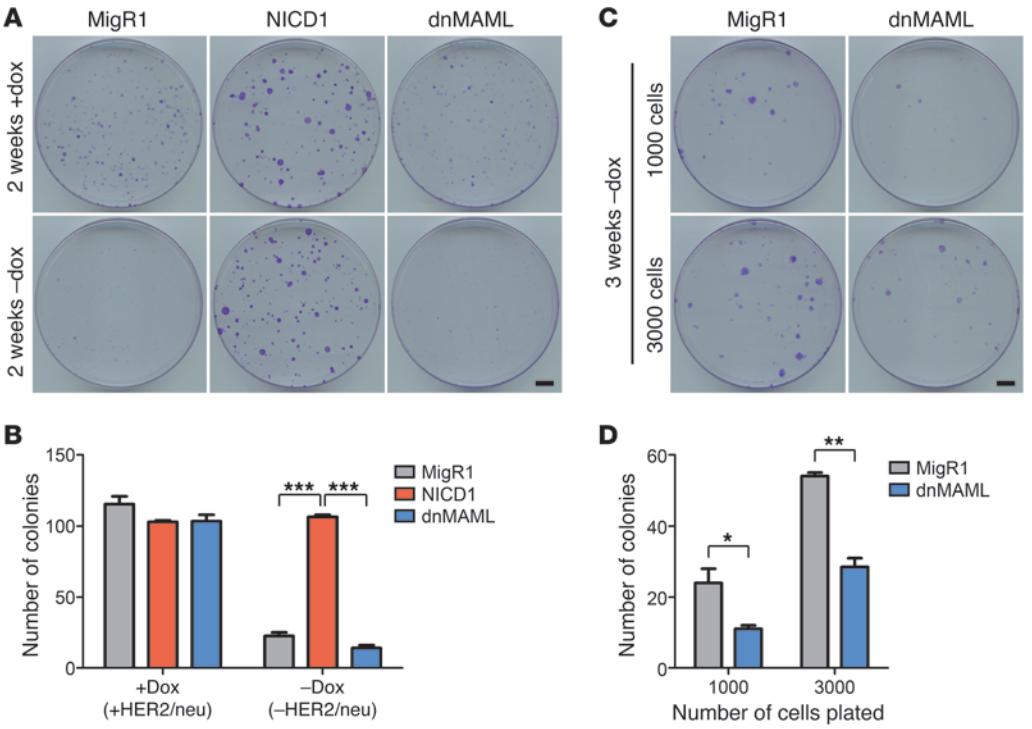

Figure 4. Notch signaling promotes colony formation following HER2/neu downregulation. (**A**) Representative clonogenic survival of primary *MTB/TAN* tumor cells transduced with vector control (MigR1), NICD1, or dnMAML expression constructs grown in the presence or absence of doxycycline for 2 weeks. (**B**) Quantification of the number of colonies in **A**. (**C**) Clonogenic survival of primary *MTB/TAN* tumor cells transduced with dnMAML expression construct or MigR1 grown in the absence of doxycycline for 3 weeks. (**D**) Quantification of the number of colonies in **C**. Scale bar: 1 cm. Data in **B** and **D** are shown as the mean ± SD. *$P < 0.05$, **$P < 0.01$, and ***$P < 0.001$ by 1-way ANOVA followed by the Bonferroni multiple comparisons test; $n = 3$.

primary tumors that overexpressed NICD1 was dramatically accelerated compared with control tumors (Figure 5A; hazard ratio [HR] 21.8, 95% confidence interval [CI] 8.26–57.7; $P < 0.0001$). This demonstrates that Notch signaling is sufficient to promote mammary tumor recurrence following HER2/neu downregulation.

We then adapted this model to permit Notch pathway inhibition by excision of floxed alleles of the canonical Notch effector *Rbpj* (48, 49). Individual *MTB/TAN* primary tumors were digested to yield single-cell suspensions, infected with Cre or GFP adenovirus (AdCre and AdGFP), and orthotopically injected into recipient mice without intervening culture. Expression of Cre in control tumor cells isolated from mice with WT *Rbpj* alleles did not alter primary orthotopic tumor growth, time to regression, or time to recurrence; these findings supported the feasibility of this experimental approach (Supplemental Figure 7, A–C).

As anticipated, AdCre infection of primary tumor cells derived from *MTB/TAN/Rbpj*$^{fl/fl}$ mice resulted in knockdown of *Rbpj* expression in primary orthotopic tumors (Supplemental Figure 7, D and E). Although *Rbpj* knockdown did not alter primary tumor growth (Supplemental Figure 7F), it markedly inhibited tumor recurrence (Figure 5B; HR 0.30, 95% CI 0.10–0.91; $P = 0.03$).

While knockdown of *Rbpj* impaired recurrence, a subset of tumors in this group recurred despite treatment with AdCre. To evaluate the mechanism by which these tumors recurred, we interrogated the RBPJ status of the resulting recurrent tumors. We found that expression of the excised *Rbpj*$^{fl/fl}$ allele (*RbpjΔ*) was lost in recurrent tumors arising from AdCre-infected tumor cells (Supplemental Figure 8A). Consistent with this, IHC for RBPJ revealed many fewer RBPJ-expressing cells in primary tumors treated with AdCre than in tumors treated with AdGFP, but little difference in the frequency of RBPJ-expressing cells in recurrent tumors treated with AdCre versus treated with AdGFP (Supplemental Figure 8B). These data suggest that strong selection pressure exists for maintaining Notch signaling during the process of recurrence but does not exclude the possibility of escape through alternative signaling pathways. In aggregate, our experiments demonstrate that activation of Notch signaling is a rate-limiting step in tumor recurrence in vivo following HER2/neu downregulation.

GSI treatment prevents recurrence of dormant MRD by blocking Notch signaling. Having established that constitutive activation of Notch signaling promotes recurrence, and that constitutive inhibition of Notch signaling delays recurrence, we used a GSI in the *MTB/TAN* mouse model of autochthonous HER2/neu driven tumor formation to dissect the role of Notch signaling during each phase of tumor progression (Figure 6A). To assess a role for Notch signaling in primary tumor formation or growth, GSI treatment was initiated either concurrently with HER2/neu activation induced by doxycycline or after primary tumors had arisen in the presence of HER2/neu signaling. Consistent with our results above regarding the lack of effects of *Rbpj* deletion on primary tumor formation, GSI treatment did not alter primary tumor latency or growth (Supplemental Figure 9).

The kinetics of tumor recurrence in women with breast cancer (2–5), along with studies of DTCs (7, 8), have suggested that

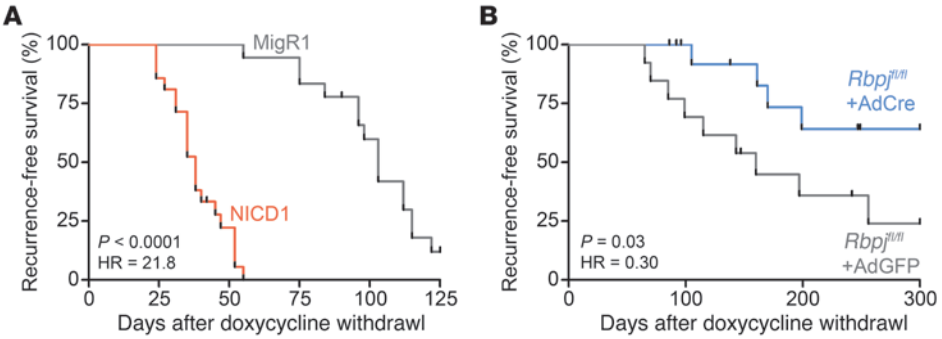

Figure 5. Notch signaling promotes tumor recurrence following HER2/neu downregulation. (**A**) Kaplan-Meier survival curves showing recurrence-free survival for mice harboring *MTB/TAN* orthotopic tumors expressing NICD1 (n = 18) or MigR1 (n = 21) constructs: HR = 21.8, 95% CI 8.26–57.7; $P < 0.0001$ by the Mantel-Haenszel method. (**B**) Kaplan-Meier survival curves showing recurrence-free survival for mice harboring orthotopic tumors generated from uncultured primary *MTB/TAN/Rbpj*$^{fl/fl}$ tumor cells infected with AdGFP (n = 13) or AdCre (n = 15): HR 0.30, 95% CI 0.10–0.91; $P = 0.03$ by the Mantel-Haenszel method.

recurrent breast cancers in patients may arise from a dormant population of residual tumor cells. In an analogous manner, we have found that *MTB/TAN* mice in which tumors have regressed to a nonpalpable state following HER2/neu downregulation harbor a residual population of dormant, Ki-67–negative, and BrdU-resistant tumor cells (refs. 13, 16, and our unpublished observations). Therefore, to address the role of Notch signaling in dormant tumor cells, we initiated GSI treatment in a cohort of mice bearing dormant residual disease generated from primary tumors that had fully regressed to a nonpalpable state following doxycycline withdrawal and HER2/neu downregulation. GSI treatment of mice bearing dormant residual tumor cells resulted in a dose-dependent inhibition of recurrence (Figure 6B; HR 0.37, 95% CI 0.15–0.94, $P = 0.037$ for 150 mg/kg GSI; HR 0.28, 95% CI 0.10–0.78, $P = 0.015$ for 300 mg/kg GSI) of a magnitude similar to that observed after constitutive knockdown of RBPJ expression throughout tumor progression.

To address the possibility that the suppressive effect of GSI treatment on tumor recurrence was due to inhibition of recurrent tumor cells that had already re-entered the cell cycle, rather than to an effect of GSI treatment on dormant residual tumor cells, control experiments were performed in which GSI treatment was not initiated until recurrent tumors had been detected. GSI treatment of existing recurrent tumors did not alter recurrent tumor growth rates (Supplemental Figure 10 and data not shown).

As γ-secretase is necessary for ligand-dependent Notch signaling, these findings suggest that while endogenous Notch signaling may not be required for the growth of primary or recurrent tumors, it does affect a rate-limiting step in tumor recurrence from dormant residual tumor cells. Consistent with a role for Notch signaling in dormant tumor cells, analysis of residual neoplastic lesions in mice bearing fully regressed tumors 28 days following HER2/neu downregulation revealed the presence of a subset of residual tumor cells with positive nuclear staining for NICD1 that was abrogated by GSI treatment (Figure 6C). This indicates that Notch signaling remains active within a subpopulation of residual tumor cells that survive HER2/neu downregulation for extended periods of time.

Since Notch receptors are not the only known substrates of γ-secretase, we wished to address whether the inhibitory effects of GSI on recurrence were Notch dependent or Notch independent. This was accomplished by performing a rescue experiment in which we determined the impact of GSI treatment on the recurrence of tumors expressing a GSI-insensitive allele of NICD1.

As above, primary HER2/neu-dependent tumor cells expressing control or NICD1 constructs were orthotopically injected into *nu/nu* mice maintained on doxycycline. Following primary tumor formation, weekly treatment with 300 mg/kg GSI or vehicle control was initiated at the time of doxycycline withdrawal to induce tumor regression. Consistent with our previous results (Figure 5A), in cohorts treated with vehicle alone, NICD1 expression dramatically accelerated the rate of recurrence compared with vector control (Figure 6D; HR 10.0, 95% CI 3.64–27.39, $P < 0.0001$). Also confirming prior results (Figure 6B), in cohorts bearing tumors transduced with the vector control, GSI treatment prevented recurrence in a substantial fraction of mice, compared with vehicle alone (Figure 6D; HR 0.23, 95% CI 0.08–0.68; $P = 0.008$).

These experiments also showed that NICD1 expression rescued the inhibitory effects of GSI treatment on recurrence. Specifically, GSI treatment did not prolong recurrence-free survival in mice bearing NICD1-expressing tumors compared with mice treated with vehicle control, and NICD1 expression accelerated recurrence compared with vector control, even in the presence of GSI (Figure 6D; HR 25.47, 95% CI 7.94–81.69, $P < 0.0001$). These findings suggest that the inhibitory effects of GSI treatment on tumor recurrence are attributable to GSI-mediated inhibition of the Notch pathway.

GSI treatment reduces MRD burden. In light of these results, we hypothesized that Notch signaling might contribute to the survival of dormant residual tumor cells. If true, this hypothesis would predict that Notch pathway inhibition in mice bearing dormant MRD would result in a reduction in the burden of dormant residual tumor cells. To test this hypothesis, we constitutively expressed Renilla luciferase in primary *MTB/TAN* tumor cells and injected these cells into the mammary fat pads of recipient *nu/nu* mice to enable the use of in vivo optical imaging to longitudinally monitor disease burden. As in the preceding experiments, doxycycline treatment was used to induce HER2/neu expression and drive primary tumor formation followed by doxycycline withdrawal in order to model tumor regression induced by HER2/neu-targeted therapy. Luciferase imaging was used to measure disease burden prior to doxycycline withdrawal and twice per week thereafter.

As expected, while doxycycline withdrawal resulted in marked tumor regression and a dramatic reduction in disease burden, residual luciferase-expressing tumor cells persisted in the mammary gland (Figure 7A). Four weeks after doxycycline withdrawal — a point at which regression was complete and the burden of dormant residual disease had stabilized — mice were randomized to receive weekly treatments with vehicle or 300 mg/kg GSI for 12

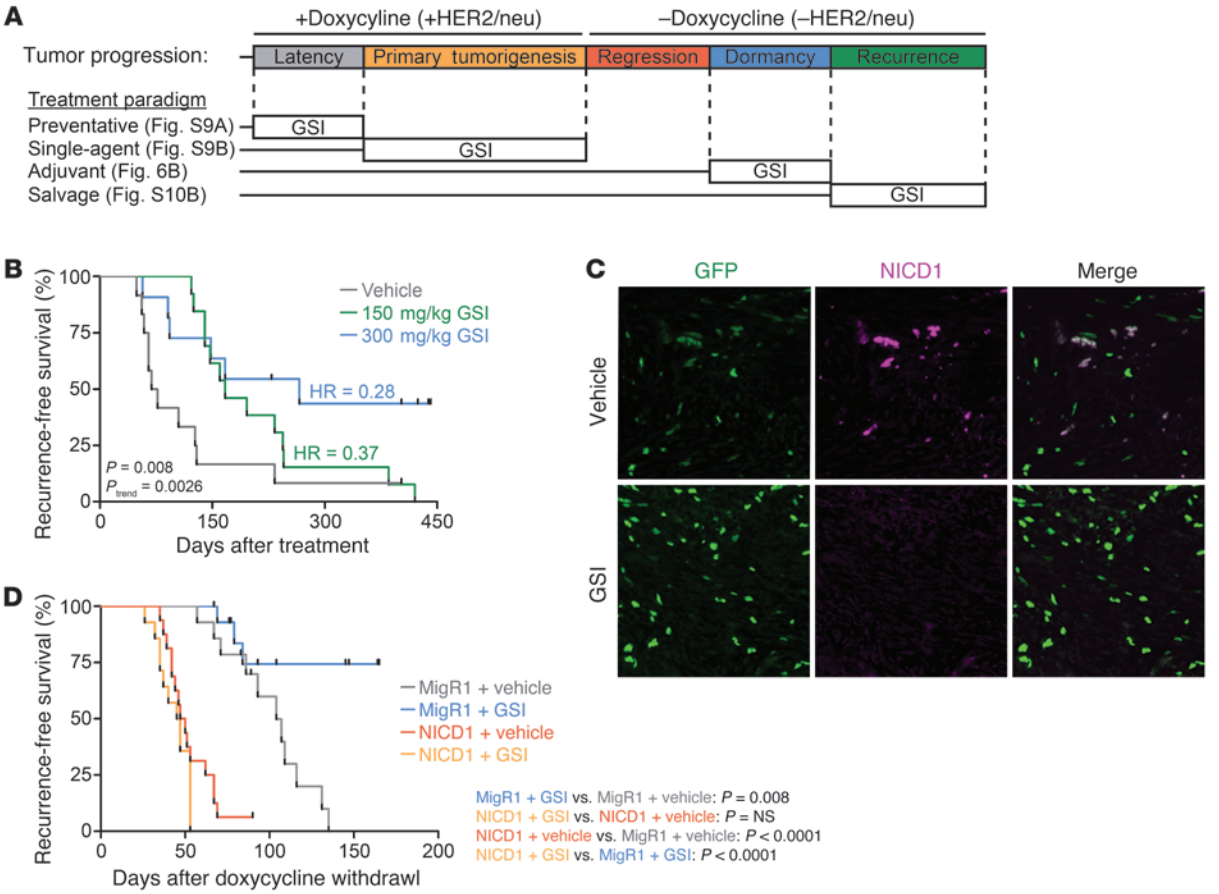

Figure 6. GSI treatment blocks recurrence of dormant residual tumor cells. (**A**) Schematic of *MTB/TAN* tumor progression and treatment paradigms. (**B**) Kaplan-Meier survival curves showing recurrence-free survival of *MTB/TAN* mice after treatment with vehicle (n = 12), 150 mg/kg (n = 13) or 300 mg/kg GSI (n = 11) initiated during tumor dormancy: HR 0.37, 95% CI 0.15–0.94, P = 0.037 for 150 mg/kg; HR 0.28, 95% CI 0.10–0.78, P = 0.015 for 300 mg/kg. (**C**) Representative immunofluorescence analysis of NICD1 in GFP$^+$ dormant residual tumor cells in mice, 28 days following HER2/neu downregulation and 24 hours after treatment with GSI or vehicle (×40 original magnification; n = 3). (**D**) Kaplan-Meier survival curves showing recurrence-free survival for mice harboring *MTB/TAN* orthotopic tumors expressing NICD1 or MigR1 constructs treated with GSI or vehicle initiated with doxycycline withdrawal: MigR1+GSI (n = 16) vs. MigR1 + vehicle (n = 14): HR 0.23, 95% CI 0.08–0.68, P = 0.008; NICD1+GSI (n = 14) vs. NICD1 + vehicle (n = 16): P = NS; NICD1 + vehicle vs. MigR1 + vehicle: HR 10.0, 95% CI 3.64–27.39, P < 0.0001; NICD1+GSI vs. MigR1+GSI: HR = 25.47, 95% CI 7.94–81.69, P < 0.0001. P values calculated by the Mantel-Haenszel method and log-rank test for trend.

weeks. Longitudinal luciferase imaging revealed that, while residual disease remained stable in vehicle-treated mice, GSI treatment of mice bearing MRD resulted in a reduction in luciferase signal (Figure 7, B–D). Since prior studies have revealed that residual tumor cells do not proliferate during this time frame, this finding implies that GSI treatment results in a decrease in the burden of dormant residual tumor cells. We cannot exclude the possibility that the decrease in luciferase signal was due to a factor other than a decreased number of residual tumor cells, such as a change in the size or distribution of tumor cells; however, in light of our findings that GSI treatment inhibits tumor recurrence only when administered during the dormant phase of tumor progression, these data are consistent with the hypothesis that Notch signaling contributes to the maintenance of MRD.

Discussion

Since recurrent breast cancer is typically incurable, the propensity of breast cancers to recur following surgery, chemotherapy, and hormonal therapy is the most important determinant of clinical outcome. However, while tumor dormancy and recurrence are responsible for the majority of breast cancer deaths, the mechanisms underlying these critical stages of cancer progression are largely unknown. Here, we demonstrate that Notch signaling plays an important role in tumor recurrence following HER2/neu inhibition. Specifically, we found that Notch activity is positively associated with breast cancer recurrence in patients and that Notch activation is sufficient to promote the recurrence of HER2/neu-driven mammary tumors in genetically engineered mice. Furthermore, we demonstrated that endogenous Notch signaling is upregulated in response to HER2/neu downregulation and is rate-limiting for tumor recurrence. Consistent with this, pharmacologic inhibition of Notch signaling suppressed tumor recurrence when administered to mice bearing dormant MRD and reduced residual disease burden following HER2/neu blockade in a manner suggestive of a reduction in the number of residual tumor cells.

Recent large-scale sequencing and screening approaches have identified recurrent Notch gene rearrangements (22), implicated Notch signaling in therapeutic resistance (28), and reinvigorated

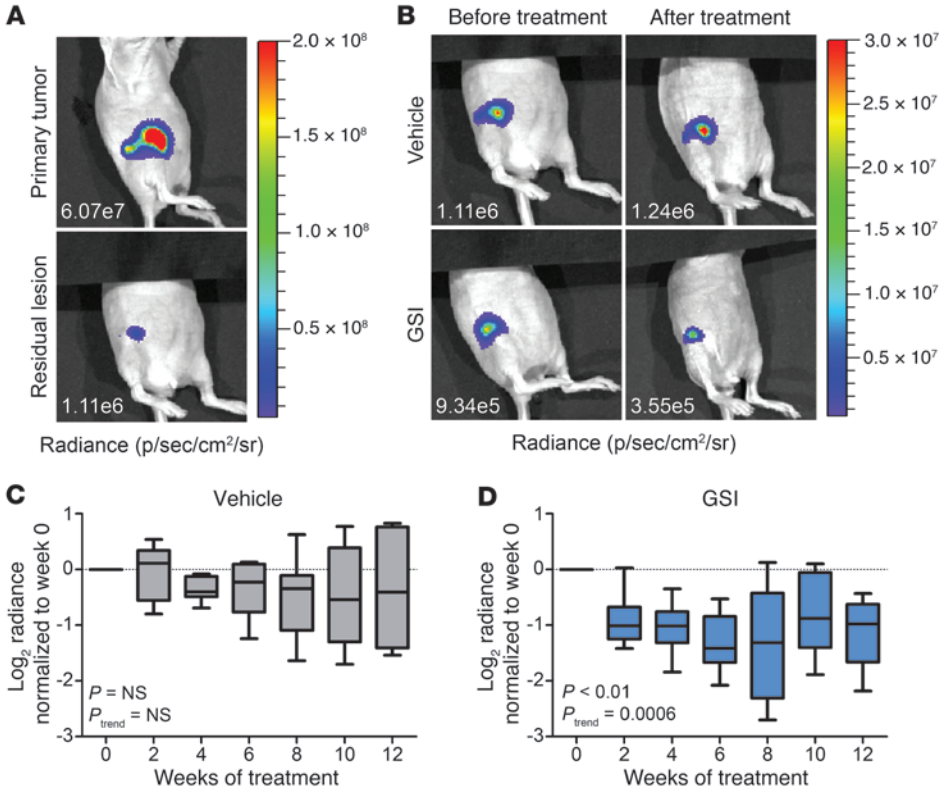

Figure 7. Inhibition of Notch signaling in mice reduces the burden of dormant MRD. (**A** and **B**) Representative images from in vivo luciferase imaging of mice bearing (**A**) primary tumors or minimal residual neoplastic lesions or (**B**) minimal residual neoplastic lesions at time points before and after treatment with vehicle or GSI. The average radiance values for each image are shown. (**C** and **D**) Box-and-whisker plots of paired longitudinal analyses of luciferase imaging in mice bearing residual lesions after treatment with (**C**) vehicle (n = 7) or (**D**) GSI (n = 6), normalized to pretreatment values. The boxes extend from the 25th–75th percentiles, with the line in the middle of each box plotted at the median. The whiskers are drawn based on the Tukey method. P values calculated by repeated-measures ANOVA.

interest in the role of Notch signaling in breast cancer pathogenesis. Notably, while these and other studies have focused on Notch signaling in primary tumors, we found that the requirement for Notch signaling during the process of tumor recurrence was specific to the stage of dormancy. While conflicting reports exist as to whether Notch signaling plays a role in the growth of HER2/neu-driven primary tumors (37, 38, 50–53), neither genetic nor pharmacologic inhibition of Notch signaling prevented primary tumor formation or suppressed the growth of HER2/neu-induced primary tumors in *MTB/TAN* mice. Indeed, we found that HER2/neu activation in primary tumor cells inhibited Notch signaling, suggesting that the Notch pathway is unlikely to play a dominant role in the growth of tumors driven by HER2/neu. In addition, not only was Notch inhibition ineffective in preventing or slowing the growth of primary tumors, but it also failed to slow the growth of tumors after they recurred. These data imply that while Notch signaling may contribute to the maintenance of dormant tumor cells, the growth of recurrent tumors is unlikely to be Notch dependent once residual cells have re-entered the cell cycle.

Breast cancers that recur most often do so as disseminated metastatic disease that can be treated but not cured. For this reason, preventing breast cancer recurrence by depleting the reservoir of dormant residual tumor cells that can give rise to recurrent tumors represents an attractive approach to this critical clinical problem. Unfortunately, dormant tumor cells are generally thought to be resistant to chemotherapeutic agents that preferentially kill proliferating cells. In this regard, our data suggest that Notch may provide a critical compensatory signaling pathway through which dormant tumor cells survive after therapy and that this pathway can be effectively targeted pharmacologically to prevent recurrence. While it is currently unclear whether drugs targeting the Notch pathway will impair the growth of established primary or recurrent metastatic tumors, their use as adjuvant agents in the setting of dormant MRD — or in the neoadjuvant setting in combination with HER2/neu-targeted therapies — could enable the elimination of dormant residual cancer cells and, consequently, could enable the prevention of recurrence.

Methods

Human breast cancer microarray data. Publicly available microarray data for 4,463 patients contained within 17 human primary breast cancer data sets (54–69), along with the corresponding clinical annotations, were downloaded from NCBI GEO or authors' websites. Microarray data were converted to base 2 logarithmic scale where necessary. Affymetrix microarray data were renormalized using Robust Multi-array Average (RMA; ref. 70) when CEL files were available.

RNA isolation and gene-expression profiling. RNA was isolated from tumors and cells using Trizol (Ambion) or RLT (QIAGEN) followed by RNeasy columns (QIAGEN). For qRT-PCR, 1 or 2 μg of RNA was reversed transcribed using high-capacity cDNA synthesis reagents (Applied Biosystems). qRT-PCR was performed on Applied Biosystems 7900 HT Fast and ViiA 7 Real-Time PCR systems using the following 6-carboxyfluorescein–labeled TaqMan probes: *Dll1* (Mm00432841_m1), *Hey1* (Mm00468865_m1), *Hey2* (Mm00469280_m1), *Errb2* (Rn00566561_m1), *Notch1* (Mm00435245_m1), *NOTCH1* (Hs01062014_m1), *Nrarp* (Mm00482529_s1), *Tbp* (Mm00446973_m1), and custom *NRARP* cDNA (Forward: CCGGAGGGCCAGACA; Reverse: GCTTCACCAGCTCCAGGTT; Probe: ACACCAGTCAGTCATCG).

For microarray profiling, all samples were processed by the University of Pennsylvania Molecular Profiling Core. RNA integrity was

analyzed using the 2100 Bioanalyzer (Agilent Technologies). Samples were reverse transcribed and labeled using the GeneChip 3′ IVT Express Kit (Affymetrix). The resulting cRNA was hybridized to Affymetrix Mouse genome 430 2.0 arrays. Raw microarray data were normalized by RMA using the Bioconductor affy package in R version 2.15.1. MAS5 detection calls were generated using the same package. Probe sets with absent detection calls in all samples or with a dynamic range of less than 1.2-fold across all samples were removed from downstream analysis. Probe set-to-gene mapping was performed in R using the Bioconductor annotation packages. For multiple probe sets mapping to the same gene, only the probe set with the highest percentage-present call was retained, with ties broken by choosing the probe set with the highest median expression across samples. Normalized gene expression data are deposited in NCBI Gene Expression Omnibus (GEO) under the accession number GSE51628.

Tissue culture and colony formation assays. *MTB/TAN* primary tumor cells were derived and grown at 37°C in 5% CO_2 as described (16) and were cultured in DMEM with 10% super calf serum, 1% Penicillin/Streptomycin, and 1% L-glutamine supplemented with 10 μg/ml EGF, 5 μg/ml insulin, 1 μg/ml hydrocortisone, 5 μg/ml prolactin, 1 μM progesterone, and 2 μg/ml doxycycline to maintain HER2/neu expression. SKBR3 cells were purchased from ATCC and cultured as recommended.

Measurements of cell viability and cell number were performed by staining with trypan blue and counting on a ViCell cell counter (BD Biosciences). For colony formation assays, 1,000 cells were plated on a 10-cm dish in complete growth medium. The next day, doxycycline was withdrawn to induce HER2/neu downregulation. Colonies were allowed to form for 2–3 weeks, after which they were fixed and stained with crystal violet for visualization and manual quantification.

Drug treatments. MRK-003 GSI was provided by Merck & Co. Inc. and was dissolved in DMSO for in vitro studies. For in vivo studies, MRK-003 was resuspended in 0.5% methycellulose vehicle and administered by oral gavage once per week. Lapatinib (B-Bridge International Inc.), MK-2206 AKTi-1/2/3 (Selleck Chemicals), PD0325901 MEKi-1/2 (Sigma-Aldrich), and SCH772984 ERKi-1/2 (Selleck Chemicals) were dissolved in DMSO for in vitro studies.

Western blotting. Western blotting was performed as described (16) using the following antibodies (obtained from Cell Signaling Technology, unless otherwise noted): NICD1 (1:1000, D3B8), NOTCH1^{NTM} (1:1,000, D6F11), HER2/ErbB2 (1:1,000, 29D8), HES1 (1:1,000, D6P2U), RBPJ (1:1,000, D10A4), pERK1/2 (1:2,000, D13.14.4E), pAKT (1:2,000, D9E), GAPDH (1:1,000, 14C10), and β-tubulin (1:2,000, BioGenex, MU122-UC). Secondary antibodies conjugated to Alexa fluor 680 (1:10,000, Invitrogen) or IRDye 800 (1:5,000, LI-COR Inc.) were detected and quantified with the Odyssey CLx Infrared Imaging System and Image Studio software (LI-COR Inc.). Secondary antibodies conjugated to HRP (Jackson ImmunoResearch Laboratories Inc.) were developed with Luminata Classico Western HRP substrate (Millipore) and exposed to film (Amersham or Kodak).

Plasmids and retrovirus production. MigR1, MigR1-NICD, and MigR1-dnMAML retroviral constructs were provided by Warren Pear. HES1 and NRARP cDNAs encoding the full-length mouse proteins were amplified by RT-PCR from primary MTB/TAN tumor cells and cloned into the pCRII-TOPO vector (Invitrogen) using the following primers: *Hes1* Forward: ATGCCAGCTGATATAATGGAGA; *Hes1* Reverse: TCAGTTCCGCCACGGTCT; NRARP Forward ATGAGCCAAGCCGAGCTGTCCACCT; and *Nrarp* Reverse: TCACCGGCCGCTGGCCGCGTA. Retroviral expression constructs were generated by subcloning *Hes1* and *Nrarp* into pK1. For luciferase expression, Renilla luciferase (RLuc) was subcloned from pRL-CMV (Promega) into MigR1.

Retrovirus was produced by transfecting the packaging line plat-E (71) with retroviral constructs using Lipofectamine 2000 (Invitrogen). Retroviral supernatant was collected 48 hours after transfection, was filtered, and was used to transduce cells in the presence of 4 μg/ml polybrene (Sigma-Aldrich). Cells were selected using puromycin or fluorescence-activated cell sorting.

Animals and recurrence assays. Animal care and experiments were performed with the approval of, and in accordance with, guidelines of the University of Pennsylvania IACUC. Mice were housed under barrier conditions with 12-hours light/12-hours dark cycles and access to food and water ad libitum. *TICNX* mice were engineered by subcloning an NICD1 construct (gift from Warren Pear) downstream of the *tet* operator sequences in the TMILA plasmid (14). Founder lines were generated by injecting the linearized construct into fertilized oocytes harvested from super-ovulated FVB/N mice and crossed with *MTB* mice (12). Mice were generated, induced with doxycycline, and sacrificed as described (12, 13).

Tumor recurrence assays were performed as described (13, 16). Briefly, for orthotopic experiments, 1×10^6 cells were injected into the inguinal mammary fat pads of female *nu/nu* mice maintained on 2 mg/ml doxycycline in their drinking water. Mice were monitored for tumor formation twice weekly. Once primary tumor endpoints were reached, doxycycline was removed to initiate oncogene downregulation and tumor regression. Mice were palpated twice weekly to monitor for tumor recurrence.

For *Rbpj* knockdown experiments, $Rbpj^{fl/+}$ mice were obtained from RIKEN BRC, backcrossed onto an FVB background, and then interbred with *MTB/TAN* mice to generate *MTB/TAN/*$Rbpj^{fl/fl}$ progeny. Primary tumor formation was induced by doxycycline treatment. To generate a single-cell suspension, tumors were manually minced and then digested in MEGM (Lonza), 1X B-27 (Invitrogen), 20 ng/ml bFGF (Sigma-Aldrich), 4 μg/ml heparin (StemCell Technologies Inc.), 5% Super Calf Serum (Gemini Bio-Products), and 1X Collagenase/Hyaluronidase (StemCell Technologies Inc.) for 1 hour at 37°C. Red blood cells were removed by suspension in red blood cell lysis buffer for 5 minutes. Cells were counted, resuspended in media with 2% serum, and infected with Ad5CMV-eGFP or Ad5CMV-Cre (University of Iowa Gene Transfer Vector Core) at an MOI of 100 for 2 hours at 37°C. Following infection, cells were washed and used for orthotopic injections.

For GSI treatment experiments, bitransgenic female *MTB/TAN* mice were generated, induced with doxycycline, monitored for tumor development, and sacrificed as described (12, 13). Mice were randomly assigned to 4 different experimental cohorts in which treatment was administered once per week, initiated at the time of doxycycline induction, primary tumor detection, full tumor regression, or recurrent tumor detection; treatment continued until humane tumor endpoints were reached. Each cohort contained 3 different treatment arms: 150 mg/kg GSI, 300 mg/kg GSI, or vehicle control. Mice were randomized between treatment cohorts by cage.

NICD immunofluorescence. GFP-labeled orthotopic tumors were generated from *MTB/TAN* cells expressing H2B-eGFP. Following primary tumor formation, doxycycline was withdrawn to induce tumor regression. Mice were treated with a single dose of vehicle or GSI 28 days after deinduction and sacrificed 24 hours later. Mammary tumors

were fixed in 4% PFA overnight, dehydrated, and embedded in paraffin blocks following standard protocols.

Paraffin tissue sections, which were 8 μm thick, were prepared using a standard xylene-based dewaxing procedure. Sections were subjected to antigen retrieval in a 2100 Retriever using Buffer A (Electron Microscopy Sciences). Slides were blocked in 5% BSA and 10% normal goat serum for 1 hour before overnight incubation at 4°C with primary antibodies. After washing, slides were incubated with secondary Alexa-Fluor–conjugated antibodies for 1 hour at 1:1000 (Invitrogen) followed by Hoechst to visualize nuclei. Anticleaved Notch1 (Cell Signaling Technology, D3B8) was used at 1:200, and Anti-GFP (Novus Biologicals, NB100-1770) was used at 1:1000.

RBPJ PCR and IHC. AdGFP- and AdCre-treated primary and recurrent orthotopic tumors were generated from *MTB/TAN/Rbpj*$^{fl/fl}$ mice as described, fixed in 4% PFA overnight, dehydrated, and embedded in paraffin blocks following standard protocols. For PCR, genomic DNA was purified from paraffin sections using the QIAamp DNA FFPE Tissue Kit (QIAGEN). *RbpjΔ* was amplified with the following primers using standard PCR protocols: *RbpjΔ* Forward: CCTTGGTTTGTTGTTTGGGTT and *RbpjΔ* Reverse: GTGGCTCTCAACTCCCAATCGT.

IHC was performed using the VECTASTAIN ABC System (Vector Laboratories). Briefly, 8-μm thick paraffin tissue sections were prepared using a standard xylene-based dewaxing procedure. Sections were subjected to antigen retrieval in a 2100 Retriever using Buffer A (Electron Microscopy Sciences). Slides were treated with H_2O_2 and blocked in 10% normal goat serum for 30 minutes before overnight incubation at 4°C with an anti-RBPJ primary antibody (D10A4, Cell Signaling Technology) at 1:1000. After washing, slides were incubated with a secondary biotinylated goat anti-rabbit antibody (BA-1000, Vector Laboratories) at 1:300 for 1 hour and developed following the kit protocol. Slides were counterstained with hematoxylin following standard protocols.

In vivo luciferase imaging. Luciferase-labeled orthotopic tumors were generated from *MTB/TAN* primary tumor cells transduced with MigR1-RLuc. Following primary tumor formation, doxycycline was withdrawn to induce tumor regression. Mice were imaged once before deinduction and then twice per week thereafter. After 28 days of deinduction, once-weekly treatment with vehicle or GSI was initiated. Mice were randomized between treatment cohorts by cage. For imaging, mice were anesthetized using isoflurane and administered 100 μl CTZ-SOL (2.5 μg/μl), a water-soluble formulation of native Coelenterazine (NanoLight Technologies) by i.v. injection. Bioluminescence images were taken immediately after substrate injection using the IVIS Spectrum (PerkinElmer). Peak signal intensity was quantified using Living Image 4.3 software (PerkinElmer).

Statistics. Two-tailed Student's *t* tests (72) were used to assess differences between 2 groups, substituting the Mann-Whitney *U* test (73) when data did not follow a normal distribution, as determined by the Shapiro-Wilk test (74). For multiple comparisons, 1-way or 2-way ANOVA was followed with Dunnett's multiple comparisons test (75), the Bonferroni multiple comparisons test (76), or the post hoc test for linear trend. The repeated-measures ANOVA was used for paired analyses, and the Geisser-Greenhouse method (77) was used to correct for violations of the sphericity assumption. Survival curves were created using the Kaplan-Meier method (78), with *P* values and hazard ratios calculated by the Mantel-Haenszel method (79) and log-rank test for trend. All tests were performed using Prism software (GraphPad Software). $P < 0.05$ was considered indicative of statistical significance. In vitro analyses are representative of at least 3 independent experiments.

To estimate relative Notch pathway activity in human breast cancer samples, we generated a Notch signature containing 72 genes concordantly regulated in 2 gene-expression microarray data sets: mammary glands from *MTB/TICNX* mice induced with doxycycline for 96 hours (data are deposited in NCBI GEO under the accession number GSE51628) and human breast cancer cell lines with and without activating *NOTCH1* gene rearrangements (22) profiled in the Cancer Cell Line Encyclopedia (CCLE; GSE36133, ref. 31). Signature genes were selected from genes common to the 2 platforms used in the above data sets with cross-species gene mapping performed using data from NCBI HomoloGene (https://www.ncbi.nlm.nih.gov/homologene).

Differentially regulated genes in the *MTB/TICNX* experiment were determined using Cyber-T (80) with a false discovery rate (81) of less than 0.01 and an absolute fold change of greater than 1.5 between the *MTB/TICNX* mice and the *TICNX* controls. In CCLE breast cancer cell lines, expression of each gene was used to rank breast cancer cell lines and then to calculate a rank-sum statistic defined as the sum of the ranks for positive cell lines with activating *NOTCH1* gene rearrangements. The significance of each rank sum was determined by its location in the distribution of rank sums from 10,000 random permutations of the ranks. Genes with rank sums in the top or bottom 2.5% of the distribution were considered as being significantly associated with NOTCH1 activation. Among the 58 breast cancer cell lines, HCC1599 and HCC2218 were considered as having activating *NOTCH1* gene rearrangements (22); 9 cell lines (DU4475, HCC1187, HS578T, MDAMB468, MCF7, ZR751, CAL51, MDAMB231, and SKBR3) were excluded from the analysis due to ambiguous NOTCH1 activation status; and the remaining 46 cell lines were considered as lacking activating *NOTCH1* gene rearrangements.

We validated the 72-gene Notch signature in one in-house (GSE51628) and 3 publicly available microarray data sets — GSE20285 (33), the T-ALL subset in GSE36133 (31), and GSE5716 (36) — using a previously described scoring method for estimating pathway activity (32). Microarray data for the validation sets were RMA normalized when CEL files were available, or taken directly from GEO and converted to base 2 logarithmic scale when CEL files were not available. Signature generation and validation were performed in R version 2.15.1.

Within each publicly available human breast cancer microarray data set, the effect size of the association between estimated Notch pathway activity and 5-year relapse-free survival was estimated using hazard ratio from Cox proportional hazards regression, in which Notch pathway activity was modeled as a continuous variable. Each type of effect-size estimate was combined across data sets by meta-analysis using the inverse-variance weighting method (82). Between-study homogeneity of survival association was tested using the χ^2 test on Cochran's Q statistic (83), for which $P < 0.05$ was interpreted as evidence of significant heterogeneity. In the presence of significant heterogeneity, the random-effect model (84) was used for meta-analysis. In the absence of significant heterogeneity, the fixed-effect model (85) was used. Cox proportional hazards regression and meta-analysis were performed using the "coxph" function in the "survival" package and the "metagen" function in the "meta" packages in R version 2.15.1. For data sets in which relapse-free survival information was not available, either distant metastasis-free survival or disease-specific death information, depending on availability, was used for survival analysis.

The association between estimated Notch activity and categorical prognostic variables in human breast cancers — including ER status, HER2/neu status, lymph node status, tumor grade, and intrinsic molecular subtype — was assessed by ANOVA in pooled microarray data sets. For each categorical prognostic variable, estimated Notch activity scores were normalized against the mean scores of the same baseline group in each data set and pooled across all data sets for which the prognostic variable was available. Baseline groups used for ER status, HER2/neu status, lymph node status, tumor grade, and intrinsic molecular subtype were ER-positive, HER2/neu-negative, lymph node–positive, grade I, and the normal-like, respectively. Baseline normalization was performed by subtracting mean Notch pathway score in the baseline group from the score for each sample. For each prognostic variable significantly associated with estimated Notch activity, we assessed the association between estimated Notch activity and relapse-free survival after adjusting for the prognostic variable in multivariate Cox proportional hazards models, and we aggregated the adjusted effect sizes using meta-analysis as described above.

Since HER2/neu IHC status was not available for many of the data sets, HER2/neu status was approximated by *ERBB2* mRNA expression, as measured by microarray in a similar fashion as the Cancer Outlier Profile Analysis (86). In each data set, HER2/neu-positive and HER2/neu-negative samples were defined as being above and below a cutoff of 1.5 median absolute deviations above the median, which resulted in average specificity of 98% and sensitivity of 78% in 5 validation data sets (56, 58, 59, 66, 87). Due to the nonrandom association between ER and HER2/neu status, approximation of HER2/neu status was not attempted in data sets consisting entirely of hormone-positive or hormone-negative cancers. Assignments of intrinsic subtype were done using the PAM50 (88) classifier after expression data were median-centered for each gene.

Study approval. Animal care and experiments were performed with the approval of, and in accordance with, guidelines of the University of Pennsylvania IACUC.

Acknowledgments

We thank Warren Pear for the MigR1, MigR1-NICD1, and MigR1-dnMAML constructs; Jianping Wang for technical assistance with histolopathology; Julie Czupryna and the University of Pennsylvania Small Animal Imaging Facility for assistance with bioluminescence imaging; the University of Pennsylvania Molecular Profiling Core for microarray profiling; Martin Scott for MRK-003 (Merck & Co. Inc.); and James Alvarez for helpful discussions. These studies were supported in part by grants from the National Cancer Institute (to L.A. Chodosh), the Department of Defense Breast Cancer Research Program (to D.L. Abravanel and L.A. Chodosh), the Breast Cancer Research Foundation (to L.A. Chodosh), and the University of Pennsylvania 2-PREVENT Breast Cancer Translational Center of Excellence.

Address correspondence to: Lewis A. Chodosh, Room 612 BRB II/III, 421 Curie Boulevard, Philadelphia, Pennsylvania 19104-6160, USA. Phone: 215.898.1321; E-mail: chodosh@mail.med.upenn.edu.

1. Jemal A, Bray F, Center MM, Ferlay J, Ward E, Forman D. Global cancer statistics. *CA Cancer J Clin*. 2011;61(2):69–90.
2. Demicheli R, Abbattista A, Miceli R, Valagussa P, Bonadonna G. Time distribution of the recurrence risk for breast cancer patients undergoing mastectomy: further support about the concept of tumor dormancy. *Breast Cancer Res Treat*. 1996;41(2):177–185.
3. Saphner T, Tormey DC, Gray R. Annual hazard rates of recurrence for breast cancer after primary therapy. *J Clin Oncol*. 1996;14(10):2738–2746.
4. Karrison TG, Ferguson DJ, Meier P. Dormancy of mammary carcinoma after mastectomy. *J Natl Cancer Inst*. 1999;91(1):80–85.
5. Weiss RB, et al. Natural history of more than 20 years of node-positive primary breast carcinoma treated with cyclophosphamide, methotrexate, and fluorouracil-based adjuvant chemotherapy: a study by the Cancer and Leukemia Group B. *J Clin Oncol*. 2003;21(9):1825–1835.
6. Braun S, et al. A pooled analysis of bone marrow micrometastasis in breast cancer. *N Engl J Med*. 2005;353(8):793–802.
7. Janni W, et al. Persistence of disseminated tumor cells in the bone marrow of breast cancer patients predicts increased risk for relapse — a European pooled analysis. *Clin Cancer Res*. 2011;17(9):2967–2976.
8. Mathiesen RR, et al. Persistence of disseminated tumor cells after neoadjuvant treatment for locally advanced breast cancer predicts poor survival. *Breast Cancer Res*. 2012;14(4):R117.
9. Pantel K, et al. Differential expression of proliferation-associated molecules in individual micrometastatic carcinoma cells. *J Natl Cancer Inst*. 1993;85(17):1419–1424.
10. Pantel K, Brakenhoff RH, Brandt B. Detection, clinical relevance and specific biological properties of disseminating tumour cells. *Nat Rev Cancer*. 2008;8(5):329–340.
11. D'Cruz CM, et al. c-MYC induces mammary tumorigenesis by means of a preferred pathway involving spontaneous Kras2 mutations. *Nat Med*. 2001;7(2):235–239.
12. Gunther EJ, et al. A novel doxycycline-inducible system for the transgenic analysis of mammary gland biology. *FASEB J*. 2002;16(3):283–292.
13. Moody SE, et al. Conditional activation of Neu in the mammary epithelium of transgenic mice results in reversible pulmonary metastasis. *Cancer Cell*. 2002;2(6):451–461.
14. Gunther EJ, et al. Impact of p53 loss on reversal and recurrence of conditional Wnt-induced tumorigenesis. *Genes Dev*. 2003;17(4):488–501.
15. Boxer RB, Jang JW, Sintasath L, Chodosh LA. Lack of sustained regression of c-MYC-induced mammary adenocarcinomas following brief or prolonged MYC inactivation. *Cancer Cell*. 2004;6(6):577–586.
16. Moody SE, et al. The transcriptional repressor Snail promotes mammary tumor recurrence. *Cancer Cell*. 2005;8(3):197–209.
17. Hurley J, et al. Docetaxel, cisplatin, and trastuzumab as primary systemic therapy for human epidermal growth factor receptor 2-positive locally advanced breast cancer. *J Clin Oncol*. 2006;24(12):1831–1838.
18. Mittendorf EA, et al. Loss of HER2 amplification following trastuzumab-based neoadjuvant systemic therapy and survival outcomes. *Clin Cancer Res*. 2009;15(23):7381–7388.
19. Nakamura R, Yamamoto N, Onai Y, Watanabe Y, Kawana H, Miyazaki M. Importance of confirming HER2 overexpression of recurrence lesion in breast cancer patients. *Breast Cancer*. 2013;20(4):336–341.
20. Arteaga CL, Sliwkowski MX, Osborne CK, Perez EA, Puglisi F, Gianni L. Treatment of HER2-positive breast cancer: current status and future perspectives. *Nat Rev Clin Oncol*. 2012;9(1):16–32.
21. Rexer BN, Arteaga CL. Intrinsic and acquired resistance to HER2-targeted therapies in HER2 gene-amplified breast cancer: mechanisms and clinical implications. *Crit Rev Oncog*. 2012;17(1):1–16.
22. Robinson DR, et al. Functionally recurrent rearrangements of the MAST kinase and Notch gene families in breast cancer. *Nat Med*. 2011;17(12):1646–1651.
23. Jhappan C, et al. Expression of an activated Notch-related int-3 transgene interferes with cell differentiation and induces neoplastic transformation in mammary and salivary glands. *Genes Dev*. 1992;6(3):345–355.
24. Gallahan D, et al. Expression of a truncated Int3 gene in developing secretory mammary epithelium specifically retards lobular differentiation resulting in tumorigenesis. *Cancer Res*. 1996;56(8):1775.
25. Raafat A, Bargo S, Anver MR, Callahan R. Mammary development and tumorigenesis in

mice expressing a truncated human Notch4/Int3 intracellular domain (h-Int3sh). *Oncogene*. 2004;23(58):9401–9407.
26. Kiaris H, et al. Modulation of notch signaling elicits signature tumors and inhibits hras1-induced oncogenesis in the mouse mammary epithelium. *Am J Pathol*. 2004;165(2):695–705.
27. Hu C, Diévart A, Lupien M, Calvo E, Tremblay G, Jolicoeur P. Overexpression of activated murine Notch1 and Notch3 in transgenic mice blocks mammary gland development and induces mammary tumors. *Am J Pathol*. 2006;168(3):973–990.
28. Martz CA, et al. Systematic identification of signaling pathways with potential to confer anticancer drug resistance. *Sci Signal*. 2014;7(357):ra121.
29. Farnie G, et al. Novel cell culture technique for primary ductal carcinoma in situ: role of Notch and epidermal growth factor receptor signaling pathways. *J Natl Cancer Inst*. 2007;99(8):616–627.
30. Reedijk M, et al. High-level coexpression of JAG1 and NOTCH1 is observed in human breast cancer and is associated with poor overall survival. *Cancer Res*. 2005;65(18):8530–8537.
31. Barretina J, et al. The Cancer Cell Line Encyclopedia enables predictive modelling of anticancer drug sensitivity. *Nature*. 2012;483(7391):603–607.
32. Wertheim GB, et al. The Snf1-related kinase, Hunk, is essential for mammary tumor metastasis. *Proc Natl Acad Sci U S A*. 2009;106(37):15855–15860.
33. Mazzone M, et al. Dose-dependent induction of distinct phenotypic responses to Notch pathway activation in mammary epithelial cells. *Proc Natl Acad Sci U S A*. 2010;107(11):5012–5017.
34. Lewis HD, et al. Apoptosis in T cell acute lymphoblastic leukemia cells after cell cycle arrest induced by pharmacological inhibition of notch signaling. *Chem Biol*. 2007;14(2):209–219.
35. Tammam J, et al. Down-regulation of the Notch pathway mediated by a γ-secretase inhibitor induces anti-tumour effects in mouse models of T-cell leukaemia. *Br J Pharmacol*. 2009;158(5):1183–1195.
36. Palomero T, et al. Mutational loss of PTEN induces resistance to NOTCH1 inhibition in T-cell leukemia. *Nat Med*. 2007;13(10):1203–1210.
37. Osipo C, et al. ErbB-2 inhibition activates Notch-1 and sensitizes breast cancer cells to a γ-secretase inhibitor. *Oncogene*. 2008;27(37):5019–5032.
38. Pandya K, et al. Targeting both Notch and ErbB-2 signalling pathways is required for prevention of ErbB-2-positive breast tumour recurrence. *Br J Cancer*. 2011;105(6):796–806.
39. Komurov K, et al. The glucose-deprivation network counteracts lapatinib-induced toxicity in resistant ErbB2-positive breast cancer cells. *Mol Syst Biol*. 2012;8:596.
40. Nakayama K, Satoh T, Igari A, Kageyama R, Nishida E. FGF induces oscillations of Hes1 expression and Ras/ERK activation. *Curr Biol*. 2008;18(8):R332–R334.
41. Sato T, et al. FRS2α regulates Erk levels to control a self-renewal target Hes1 and proliferation of FGF-responsive neural stem/progenitor cells. *Stem Cells*. 2010;28(9):1661–1673.
42. Sweeney C, et al. Growth factor-specific signaling pathway stimulation and gene expression mediated by ErbB receptors. *J Biol Chem*. 2001;276(25):22685–22698.
43. Amin DN, Perkins AS, Stern DF. Gene expression profiling of ErbB receptor and ligand-dependent transcription. *Oncogene*. 2004;23(7):1428–1438.
44. Kobayashi T, Kageyama R. Hes1 regulates embryonic stem cell differentiation by suppressing Notch signaling. *Genes Cells*. 2010;15(7):689–698.
45. Lamar E, et al. Nrarp is a novel intracellular component of the Notch signaling pathway. *Genes Dev*. 2001;15(15):1885–1899.
46. Weng AP, et al. Growth suppression of pre-T acute lymphoblastic leukemia cells by inhibition of notch signaling. *Mol Cell Biol*. 2003;23(2):655–664.
47. Maillard I, et al. Mastermind critically regulates Notch-mediated lymphoid cell fate decisions. *Blood*. 2004;104(6):1696–1702.
48. Kato H, et al. Involvement of RBP-J in biological functions of mouse Notch1 and its derivatives. *Development*. 1997;124(20):4133–4141.
49. Han H, et al. Inducible gene knockout of transcription factor recombination signal binding protein-J reveals its essential role in T versus B lineage decision. *Int Immunol*. 2002;14(6):637–645.
50. Yamaguchi N, et al. NOTCH3 signaling pathway plays crucial roles in the proliferation of ErbB2-negative human breast cancer cells. *Cancer Res*. 2008;68(6):1881–1888.
51. Watters JW, et al. De novo discovery of a γ-secretase inhibitor response signature using a novel in vivo breast tumor model. *Cancer Res*. 2009;69(23):8949–8957.
52. Efferson CL, et al. Downregulation of Notch pathway by a gamma-secretase inhibitor attenuates AKT/mammalian target of rapamycin signaling and glucose uptake in an ERBB2 transgenic breast cancer model. *Cancer Res*. 2010;70(6):2476–2484.
53. Kondratyev M, et al. γ-Secretase inhibitors target tumor-initiating cells in a mouse model of ERBB2 breast cancer. *Oncogene*. 2012;31(1):93–103.
54. Chang HY, et al. Robustness, scalability, and integration of a wound-response gene expression signature in predicting breast cancer survival. *Proc Natl Acad Sci U S A*. 2005;102(10):3738–3743.
55. Chanrion M, et al. A gene expression signature that can predict the recurrence of tamoxifen-treated primary breast cancer. *Clin Cancer Res*. 2008;14(6):1744–1752.
56. Chin K, et al. Genomic and transcriptional aberrations linked to breast cancer pathophysiologies. *Cancer Cell*. 2006;10(6):529–541.
57. Desmedt C, et al. Strong time dependence of the 76-gene prognostic signature for node-negative breast cancer patients in the TRANSBIG multicenter independent validation series. *Clin Cancer Res*. 2007;13(11):3207–3214.
58. Hess KR, et al. Pharmacogenomic predictor of sensitivity to preoperative chemotherapy with paclitaxel and fluorouracil, doxorubicin, and cyclophosphamide in breast cancer. *J Clin Oncol*. 2006;24(26):4236–4244.
59. Esserman LJ, et al. Chemotherapy response and recurrence-free survival in neoadjuvant breast cancer depends on biomarker profiles: results from the I-SPY 1 TRIAL (CALGB 150007/150012; ACRIN 6657). *Breast Cancer Res Treat*. 2012;132(3):1049–1062.
60. Ivshina AV, et al. Genetic reclassification of histologic grade delineates new clinical subtypes of breast cancer. *Cancer Res*. 2006;66(21):10292–10301.
61. Ma XJ, et al. A two-gene expression ratio predicts clinical outcome in breast cancer patients treated with tamoxifen. *Cancer Cell*. 2004;5(6):607–616.
62. Curtis C, et al. The genomic and transcriptomic architecture of 2,000 breast tumours reveals novel subgroups. *Nature*. 2012;486(7403):346–352.
63. Minn AJ, et al. Lung metastasis genes couple breast tumor size and metastatic spread. *Proc Natl Acad Sci U S A*. 2007;104(16):6740–6745.
64. Oh DS, et al. Estrogen-regulated genes predict survival in hormone receptor-positive breast cancers. *J Clin Oncol*. 2006;24(11):1656–1664.
65. Pawitan Y, et al. Gene expression profiling spares early breast cancer patients from adjuvant therapy: derived and validated in two population-based cohorts. *Breast Cancer Res*. 2005;7(6):R953–R964.
66. Sabatier R, et al. A gene expression signature identifies two prognostic subgroups of basal breast cancer. *Breast Cancer Res Treat*. 2011;126(2):407–420.
67. Schmidt M, et al. The humoral immune system has a key prognostic impact in node-negative breast cancer. *Cancer Res*. 2008;68(13):5405–5413.
68. Sotiriou C, et al. Gene expression profiling in breast cancer: understanding the molecular basis of histologic grade to improve prognosis. *J Natl Cancer Inst*. 2006;98(4):262–272.
69. Wang Y, et al. Gene-expression profiles to predict distant metastasis of lymph-node-negative primary breast cancer. *Lancet*. 2005;365(9460):671–679.
70. Irizarry RA, et al. Exploration, normalization, and summaries of high density oligonucleotide array probe level data. *Biostatistics*. 2003;4(2):249–264.
71. Morita S, Kojima T, Kitamura T. Plat-E: an efficient and stable system for transient packaging of retroviruses. *Gene Ther*. 2000;7(12):1063–1066.
72. Student. The probable error of a mean. *Biometrika*. 1908;6(1):1–25.
73. Mann HB, Whitney DR. On a test of whether one of two random variables is stochastically larger than the other. *Ann Math Stat*. 1947;18(1):50–60.
74. Shapiro S, Wilk M. An analysis of variance test for normality (complete samples). *Biometrika*. 1965;52(3):591–611.
75. Dunnett CW. A multiple comparison procedure for comparing several treatments with a control. *J Am Stat Assoc*. 1955;50(272):1096–1121.
76. Dunn OJ. Multiple comparisons among means. *J Am Stat Assoc*. 1961;56(293):52–64.
77. Greenhouse SW, Geisser S. On methods in the analysis of profile data. *Psychometrika*. 1959;24(2):95–112.
78. Kaplan EL, Meier P. Nonparametric estimation from incomplete observations. *J Am Stat Assoc*. 1958;53(282):457–481.
79. Mantel N, Haenszel W. Statistical aspects of the analysis of data from retrospective studies of disease. *J Natl Cancer Inst*. 1959;22(4):719–748.
80. Baldi P, Long AD. A Bayesian framework for the analysis of microarray expression data: regularized t-test and statistical inferences of gene changes. *Bioinformatics*. 2001;17(6):509–519.

81. Benjamini Y, Hochberg Y. Controlling the false discovery rate: a practical and powerful approach to multiple testing. *J R Stat Soc B Stat Methodol*. 1995;57(1):289–300.
82. Ramasamy A, Mondry A, Holmes CC, Altman DG. Key issues in conducting a meta-analysis of gene expression microarray datasets. *PLoS Med*. 2008;5(9):e184.
83. Cochran W. The combination of estimates from different experiments. *Biometrics*. 1954;10(1):101–129.
84. DerSimonian R, Laird N. Meta-analysis in clinical trials. *Control Clin Trials*. 1986;7(3):177–188.
85. Whitehead A, Whitehead J. A general parametric approach to the meta-analysis of randomized clinical trials. *Stat Med*. 1991;10(11):1665–1677.
86. Rubin MA, Chinnaiyan AM. Bioinformatics approach leads to the discovery of the TMPRSS2: ETS gene fusion in prostate cancer. *Lab Invest*. 2006;86(11):1099–1102.
87. Popovici V, et al. Effect of training-sample size and classification difficulty on the accuracy of genomic predictors. *Breast Cancer Res*. 2010;12(1):R5.
88. Parker JS, et al. Supervised risk predictor of breast cancer based on intrinsic subtypes. *J Clin Oncol*. 2009;27(8):1160–1167.